Regular paper

Title

Kinetic properties and substrate inhibition of α-galactosidase from *Aspergillus niger*

Authors

Julan Liao, Masayuki Okuyama, Keigo Ishihara, Yoshinori Yamori, Shigeo Iki, Takayoshi Tagami, Haruhide Mori, Seiya Chiba, and Atsuo Kimura*

Affiliation

Research Faculty of Agriculture, Hokkaido University, Sapporo, Japan

*Corresponding author. E-mail: kimura@abs.agr.hokudai.ac.jp

Running title

Properties of AglB from *A. niger*

Abbreviations

BSA, bovine serum albumin; GH, glycoside hydrolase family; GM2, 6^{I}-α-D-galactosylmannobiose; GM3, 6^{I}-α-D-galactosylmannotriose; G2M5, 6^{III},6^{IV}-α-D-galactosylmannopentaose; HPAEC-PAD, high-performance anion-exchange chromatography-pulsed amperometric detection; PNPG, *p*-nitrophenyl α-galactoside; rAglB, recombinant AglB

Abstract

The recombinant AglB produced by *Pichia pastoris* exhibited substrate inhibition behavior for the hydrolysis of *p*-nitrophenyl α-galactoside, whereas it hydrolyzed the natural substrates, including galactomanno-oligosaccharides and raffinose family oligosaccharides, according to the Michaelian-kinetics. These contrasting kinetic behaviors can be attributed to the difference in the dissociation constant of second substrate from the enzyme and/or to the ability of the leaving group of the substrates. The enzyme displays the grater k_{cat}/K_m values for hydrolysis of the branched α-galactoside in galactomanno-oligosaccharides than that of raffinose and stachyose. A sequence comparison suggested that AglB had a shallow active-site pocket, and it can allow to hydrolyze the branched α-galactosides but not linear raffinose family oligosaccharides.

Keywords

glycoside hydrolase family 27, α-galactosidase, substrate inhibition, substrate specificity

Introduction

Enzymatic degradation of plant cell wall polysaccharides (cellulose, hemicellulose, and pectin) has many industrial applications, such as biofuel, paper, and food. Among these polysaccharides, the hemicelluloses, including xylan, (galacto)glucomannan, and xyloglucan, are the second most abundant organic structure in the plant cell wall after cellulose.

Galactomannan consists of a β-1,4-linked D-mannose residues backbone, which can be substituted by D-galactose residues via an α-1,6-linkage. Mannose/galactose ratios vary from 1.0 to 5.3 depending on the source of the polysaccharides. Galactoglucomannan has a similar structure to galactomannan, but the backbone consists of β-1,4-linked D-mannose and D-glucose residues. [1–3] α-Galactosidases play an important role in the degradation of galacto(gluco)mannan, catalyzing the hydrolysis of the branched α-galactosidic linkage on mannose residues. For example, α-galactosidase, glycoside hydrolase family (GH) 27, from *Cyamopsis tetragonolobus* seeds shows the ability to synergistically interact with GH26 mannanase in the hydrolysis of galactomannans, guar gum, and locust bean gum. [4]

Several α-galactosidases have been purified from *Aspergillus* sp. and these exhibit different enzymatic characteristics. [3] Three different genes that encode α-galactosidase have been cloned from *Aspergillus niger*. [5–7] Two enzymes, AglA and AglB, belong to GH27, and the third enzyme AglC belongs to GH36. AglB is known to be the major α-galactosidase involved in galactomannan degradation. [7] The enzyme catalyzes the hydrolysis of the α-galactosidic linkage though retaining mechanism, which is composed of two chemical steps, glycosylation and deglycosylation, with a galactosyl-enzyme intermediate between the two steps.

The *aglB* gene is expressed at the basal level on a wide range of carbon sources

including monosaccharides, oligosaccharides, and polysaccharides [6] but is quickly and highly expressed in response to the presence of galactomannans in a culture medium. This expression pattern is synchronous with the *mndA* gene, which encodes GH2 β-mannosidase.

In this study, we investigated an α-galactosidase derived from *A. niger*. This filamentous fungus is widely used in industry for the production of organic acids and enzymes. *Transglucosidase "Amano"* is one such enzyme preparation for producing panose and isomaltooligosaccharides from maltooligosaccharides. It is mainly composed of α-glucosidase but also contains α-galactosidase. A cDNA encoding the α-galactosidase is cloned from *A. niger* mycelia and heterologously expressed in *Pichia pastoris*. The recombinant enzyme hydrolyzes the α-galactosidic linkages in galactomanno-oligosaccharides and in raffinose family oligosaccharides such as melibiose, raffinose, and stachyose and efficiently hydrolyzes the former α-galactosidic linkages. The enzyme shows typical Michaelis-Menten kinetics for the hydrolysis of such a natural substrate, but the rate for hydrolysis of *p*-nitrophenyl α-galactoside (PNPG) differs from typical Michaelis-Menten kinetics.

Materials and Methods

cDNA cloning and construction of a recombinant expression vector plasmid.

A. niger No.499 cells, a gift from Amano Enzyme Inc., were cultivated aerobically in a corn meal (Sigma–Aldrich, St. Louis, MO, USA) infusion broth supplemented with 15 g/L corn steep liquor (Amano Enzyme Inc.), with pH adjusted to 4.9, and maintained at 30°C with rotary shaking. Total RNAs were extracted according to the hot-phenol method, [8] and poly(A)$^+$ mRNAs were isolated with Oligotex-dT30 Super (Takara Bio Inc., Otsu, Japan). First-strand cDNA was synthesized by SuperScript II reverse

transcriptase (Life Technologies, Carlsbad, CA, USA) with an extension primer (3′-AP: 5′-GGCCACGCGTCGACTAGTAC$(T)_{17}$-3′) from poly$(A)^+$ RNAs. Synthesized single-strand cDNA was amplified using Ex Taq DNA polymerase (Takara Bio) with a pair of synthesized primers: 3′-AuAP (antisense: 5′-GGCCACGCGTCGACTAGTAC-3′) and A10 (sense: 5′-ATATCCATTGAAAGCACTTGAGAA-3′), designed according to the *aglB* gene sequence (accession no. Y18586.1) of *A. niger* N400. [6] cDNA obtained was 1493 bp and encoded 443 amino acids (accession no. LC105654). One base substitution (101 T → G) was identified and it caused an amino acid substitution of Leu25 → Arg compared with the reported *aglB* cDNA of *A. niger* N400. The N-terminal amino acid sequence of the purified enzyme began from Leu17 and the N-terminal 16 amino acids encoded should be a secretion signal sequence. The recombinant AglB (rAglB) was designed to have the N-terminal peptide of the *Saccharomyces cerevisiae* α-factor secretion signal and His_6-tag at the C-terminus following the procedure below. A cDNA encoding the mature AglB (Leu17-Cys433) was amplified by polymerase chain reaction (PCR) using a sense primer (5′-CGCACAATTGGTTCGACCCGA-3′, the *Mun*I site is underlined) and an antisense primer (5′-GGCGTCTAGACCACATTGCCCTCC-3′, the *Xba*I site is underlined). This was followed by digestion with *Mun*I and *Xba*I and cloned into the *Eco*RI-*Xba*I sites of pPICZαA (Life Technologies).

Production of rAglB in P. pastoris.

Transformation of the *P. pastoris* strain GS115 was performed as described by Lin-Cereghino *et al.* [9] The above pPICZαA derivative of the expression vector plasmid (approximately 20 μg) was linearized with *Sac*I and introduced into *P. pastoris* by electroporation. Transformants were selected on YPDSZ agar plates (10 g/L yeast

extract, 20 g/L peptone, 20 g/L glucose, 1 M sorbitol, 100 μg/mL zeocin, and 20 g/L agar). The selected transformant was cultured in BMGY [3.4 g/L yeast nitrogen base without amino acids and ammonium sulfate (BD Biosciences, San Jose, CA, USA), 10 g/L ammonium sulfate, 10 g/L yeast extract, 10 g/L peptone, 1% (v/v) glycerol, 0.4 mg/L biotin, and 0.1 M potassium phosphate buffer, pH 6.0] overnight at 30°C. Cells were harvested by centrifugation for 15 min at 3000 × *g*, resuspended in BMMY (3.4 g/L yeast nitrogen base without amino acid and ammonium sulfate, 10 g/L ammonium sulfate, 10 g/L yeast extract, 10 g/L peptone, 0.5% (v/v) methanol, 0.4 mg/L biotin, and 0.1 M potassium phosphate buffer, pH 6.0), followed by incubation for 24 h at 30°C under vigorous shaking. The supernatant was obtained by centrifugation for 15 min at 8000 × *g* at 4°C.

Purification of rAglB.

The pH of the obtained supernatant was adjusted to pH 7.2 with 1 M sodium hydroxide and centrifugation (8000 × *g*, 15 min, 4°C) was performed to remove the generated debris. The supernatant was loaded onto Ni-chelating Sepharose Fast Flow (GE Healthcare) equilibrated with a starting buffer (20 mM imidazole, pH 7.2, 20 mM sodium phosphate buffer containing 500 mM NaCl, pH 7.2) followed by the washing buffer. The bound proteins were eluted with a linear gradient of 20–500 mM imidazole in the starting buffer. The active fractions were dialyzed against a 20 mM sodium acetate buffer (pH 6.0). The purified rAglB was concentrated using Centriprep YM-30 centrifugal filter units (Millipore, Billerica, MA, USA).

Biochemical assays.

The purity of rAglB was determined by SDS-PAGE. *N*-deglycosylation of the

purified rAglB with endoglycosidase H (0.25 U Roche, Basel, Switzerland) was carried out at 37°C for 16 h after the enzyme (0.1 mg/0.1 mL) was denatured by heating at 100°C for 10 min. The protein concentration of the purified enzyme was estimated by amino acid analysis of the protein hydrolysate (6 M HCl, 110°C, 24 h) using JLC-500/V (Nihon Denshi, Tokyo, Japan) equipped with a ninhydrin-detection system.

Enzyme activity was measured at 37°C in the standard mixture (200 μL) consisting of 2 mM PNPG (Nacalai tesque, Kyoto, Japan) , 50 mM sodium acetate buffer (pH 4.6), 0.1 mg/mL bovine serum albumin (BSA), and enzyme at the appropriate concentration. The reaction was stopped every 3 min by mixing an aliquot of 50 μL of the reaction mixture with 100 μL of 1 M sodium carbonate. The amount of *p*-nitrophenol released was measured by the absorption at 400 nm in a 1 cm cuvette using a one molar extinction coefficient of 5560 M^{-1} cm^{-1}. Enzyme activity was defined as the amount of enzyme hydrolyzing 1 μmol PNPG per minute under the above conditions.

The effects of temperature on PNPG hydrolysis activity were investigated under standard assay conditions at various temperatures from 25–55°C. To measure thermostability, the enzyme in 100 mM sodium acetate buffer (pH 4.4) containing 0.17 mg/mL BSA was kept at 25–55°C for 15 min, after which their residual activities under the standard assay conditions were measured. To measure pH stability, rAglB was incubated in Britton-Robinson buffer (pH 2.5–10.0) containing 0.01 mg/mL BSA at 4°C for 24 h, after which their residual activities under the standard assay conditions were measured. The stable region was defined as the pH range that exhibited a residual activity of >90%.

The kinetic parameters for hydrolysis of PNPG were calculated from the initial rates at eight substrate concentrations (0.048–2 mM) at various pH values (40 mM citrate-80 mM Na_2HPO_4 buffer) by fitting the expression for substrate inhibition;

$v/[E]_0 = k_{cat}[S]/(K_m + [S] + [S]^2/K_i)$, using KaleidaGraph 3.6J (Synergy Software, Reading, PA, USA). The rate constant obtained at each pH level were fitted to a theoretical bell shaped ionization curve: $k_{cat}/K_m = \text{limit}/\{1+10^{(pH - pKe1)} + 10^{(pKe2 - pH)}\}$

The kinetic parameters for hydrolysis of α-galactosidic linkages in melibiose, raffinose, stachyose, 6^I-α-D-galactosylmannobiose (GM2, Megazyme, Bray Ireland), 6^I-α-D-galactosylmannotriose (GM3, Megazyme), and 6^{III},6^{IV}-α-D-galactosylmannopentaose (G2M5, Megazyme) were calculated from the initial rates determined in a 40 mM citrate-80 mM Na_2HPO_4 buffer at pH 4.6. For the hydrolysis of melibiose, the liberated glucose concentration was measured with the Glucose C II-Test Wako (Wako, Osaka, Japan). For the hydrolysis of other substrates, liberated galactose was measured with the high-performance anion-exchange chromatography-pulsed amperometric detection (HPAEC-PAD). HPAEC-PAD was performed on a Dionex ICS 3000 (Dionex/Thermo Fisher Scientific, Idstein, Germany) equipped with a platinum electrode on an electrochemical detector in the pulsed amperometric mode with a CarboPac PA1 (4 × 250 mm) analytical column. The chromatograms were processed on a Chromelen system (Dionex/Thermo Fisher Scientific). The separation of each substrate reaction mixture was achieved with a sodium hydroxide gradient. The enzyme concentrations used were 3.4–41 nM. Data were fitted to the Michaelis–Menten equation using KaleidaGraph 3.6J.

Results and Discussion

Purification and characterization of rAglB.

The matured polypeptide (Leu17 to Cys433) of AglB was produced as a fusion protein with the N-terminal peptide encoding the *S. cerevisiae* α-factor secretion signal

and C-terminal His_6-tag, in *P. pastoris*. The rAglB was purified with Ni-affinity column chromatography. The specific activity of the purified enzyme was 197 U/mg. The purified enzyme showed a broad band on a SDS-PAGE gel and converged on a sharp single band with a molecular mass of 60 kDa by a treatment of endoglycosidase H (Fig. 1). The broad band could be due to the hyper-glycosylation. The amino acid sequence bears seven sequons (Asn-X-Ser/Thr) and these should be highly glycosylated. The molecular mass of 60 kDa was still slightly larger than a theoretical molecular mass calculated from the amino acid sequence including the hexa-histidine tag and its spacer sequence (51 kDa), and the rAglB could be partially modified by *O*-glycosylation.

The effects of temperature and pH on rAglB activity were investigated. The rAglB was stable for 15 min during heat treatments at temperatures up to 45°C and for 24 h between pH 3.7–7.8 at 4°C. Maximum PNPG hydrolysis rates were obtained at 45–50°C. These properties were almost identical to the native AglB except for heat-stability, which of the native enzyme was less than 36°C. To determine the optimum pH, the hydrolysis rate of 2 mM PNPG was measured at various pH levels from 3.0–7.0. The hydrolytic rates showed no bell shape and they increased with decreasing pH (Fig. 2A). This profile was rather odd because the double displacement mechanism uses two ionization groups for catalysis and a pH rate profile should display a typical bell shape.

Substrate inhibition in the hydrolysis of PNPG.

Kinetic parameters for the hydrolysis of PNPG at various pH levels were determined to investigate the pH rate profile in some detail. The hydrolytic rate departed from the Michaelis–Menten equation as displayed in Fig. 2B. These data fitted well to the substrate inhibition expression. This kinetic behavior was observed at all other pH levels that were tested (Table 1). Even though the hydrolytic rates of 2 mM

PNPG at various pH levels showed no bell shape, the pH-dependence of k_{cat}/K_m was accurately bell shaped and the obtained pK_e values were 3.0 and 6.1 (Fig. 2C). This should be because k_{cat}/K_m [$= k_1k_2/(k_{-1} + k_2)$] is never affected by the concentration of a substrate and substrate inhibition. The non-bell shaped behavior was probably thus due to the substrate inhibition behavior.

In the case of the AglB, which employs the double displacement mechanism, a substrate transglycosylation pathway should be taken into account as well as the substrate inhibition in order to explain the observed kinetic behavior because the substrate transglycosylation results demonstrate a similar kinetic behavior as the substrate inhibition behavior. [10] The ability of transglycosylation of the rAglB was investigated by using 2 mM of PNPG as the substrate. The concentration of released galactose and that of *p*-nitrophenol from the rAglB reaction were measured by HPAEC-PAD and spectrophotometric analyses, respectively. Their concentrations were almost identical and no transglycosylation product was detected on HPAEC-PAD. Therefore, the enzyme exhibited no transglycosylation, and the non-Michaelian behavior was most likely due to substrate inhibition. Although the rAglB showed substrate inhibition for the hydrolysis of PNPG, it followed the Michaelian-kinetics for hydrolysis of the natural substrates, including melibiose, raffinose, stachyose, and galactomanno-oligosaccharides as mentioned below.

This contrasting kinetic behaviors can be accounted for the difference of K_d values, which represent the dissociation constant of a second molecule of substrate from the enzyme, between PNPG and the natural substrates. In the double displacement mechanism, substrate inhibition will occur when a substrate molecule secondarily binds to a Michaelis complex (ES complex) and gives rise to a substrate-inhibited Michaelis complex (ESS complex) that is catalytically inactive (scheme 1 in Fig. 3). Furthermore,

the formation of the FS complex that turns over slowly (extremely small k_5) will also cause substrate inhibition (scheme 2 in Fig. 3). If the FS complex turns over sufficiently, transglycosylation would occur instead of substrate inhibition. The rate equations of schemes 1 and 2 are expressed as Eqs. 1 and 2, respectively.

$$\frac{v}{[\mathrm{E}]_0} = \frac{\frac{k_2 k_3}{k_2 + k_3}[\mathrm{S}]}{\frac{k_{-1} + k_2}{k_1} \cdot \frac{k_3}{k_2 + k_3} + [\mathrm{S}] + \frac{1}{K_\mathrm{d}} \cdot \frac{k_3}{k_2 + k_3}[\mathrm{S}]^2} \qquad \text{Eq. 1}$$

$$\frac{v}{[\mathrm{E}]_0} = \frac{\frac{k_2 k_3}{k_2 + k_3}[\mathrm{S}]}{\frac{k_{-1} + k_2}{k_1} \cdot \frac{k_3}{k_2 + k_3} + [\mathrm{S}] + \frac{1}{K_\mathrm{d}} \cdot \frac{k_2}{k_2 + k_3}[\mathrm{S}]^2} \qquad \text{Eq. 2}$$

where K_d is k_{-4}/k_4.

The rate equations indicate that each K_i is expressed as K_d $(k_2 + k_3)/k_3$ (scheme 1) or K_d $(k_2 + k_3)/k_2$ (scheme 2). The K_d value would be thus closely related to the strength of the inhibition in each case. It is likely that the much larger K_d value of the natural substrates than that of PNPG leads the [S] squared term to approach zero and gives the law to the Michaelian-kinetics.

Although the difference in the K_d value between PNPG and the natural substrates should contribute to the contrasting kinetic behaviors, no inhibition observed in the natural substrates can be explained by difference in rate constants, k_2 and k_3, when the K_d value of the natural substrates being comparable to that of PNPG. This is because K_i is ruled by not only K_d but also k_2 and k_3, and these rate constants can affect the substrate inhibition behavior. When $k_3 \ll k_2$ in scheme 1 and $k_2 \ll k_3$ in scheme 2 hold, the respective [S] squared term of their rate equations would be negligibly small, and thus no substrate inhibition can be observed. For hydrolysis of the natural substrates, k_2

is a rate constant for a bond cleavage step and might be much smaller than k_3. The Michaelian-behavior for hydrolysis of the natural substrates can be thus attributed to the reaction following the scheme 2. Likewise, the substrate inhibition of the hydrolysis of PNPG can be explained. If $k_2 \ll k_3$ is established for the same reason as the natural substrates, the substrate inhibition is caused by the formation of ESS (scheme 1). Meanwhile, if the reaction employs scheme 2 as is the case of the natural substrates, the substrate inhibition occurs unless $k_2 \ll k_3$ is established. The k_2 value for the hydrolysis of PNPG can be greater than that of the natural substrates because pK_a of the leaving group of PNPG is lower than that of the natural substrates: the pK_a value of *p*-nitrophenol is 7.18 and the calculated pK_a values of O6 of α- and β-glucoses, which correspond to the leaving group of melibiose, are 15.86 and 20.65, respectively. [11] It is thus possible that the k_2 value for the hydrolysis of PNPG goes close to the k_3 value and somewhat breaks down $k_2 \ll k_3$. Hence, it may allow the formation of the FS complex and cause the substrate inhibition. As mentioned above, AglB exhibited no transglycosylation using 2 mM of PNPG, and this result implied that turnover of the FS complex is too slow if the complex formed.

We favor the hypothesis that the substrate inhibition of PNPG is caused by the formation of the inert FS complex (scheme 2), as long as PNPG and the natural substrates are similar in the K_d value. PNPG with better leaving group unlikely to form the ESS complex rather than the galactosyl-enzyme intermediate (F), since even the natural substrates with poorer leaving group can be considered to form no ESS complex. A similar kinetic behavior was observed in a GH27 α-galactosidase from *Phanerocaete chrysosporium*. The enzyme hydrolyzed 1-naphtyl and 6-bromo-2-naphtyl α-galactosides and 1-fluoro α-galactosyl fluoride with poor leaving groups according to Michaelian kinetics, but the hydrolysis of *o*- and *p*-nitrophenyl α-galactosides and

α-galactosyl fluoride with good leaving groups exhibited substrate inhibition. [10] In this report, Brumer *et al*. attributed this behavior to the formation of the inert FS complex, which corresponds to scheme 2 in this study.

Although there is no definitive answer for the substrate inhibition by difference in substrate at present, the K_d values of second substrate from the enzyme, and/or the ability of the leaving groups of substrate should be related to the contrasting kinetic behaviors.

Substrate specificity of rAglB on natural substrates.

The substrate specificity was investigated by determining the kinetic parameters for hydrolysis of natural substrates, including melibiose, raffinose, stachyose, and galactomanno-oligosaccharides. The hydrolytic rates on all substrates tested conformed to the Michaelis–Menten equation. The kinetic parameters are summarized in Table 2. The rAglB was able to hydrolyze α-galactoside in the natural substrates. This broad substrate specificity of the rAglB seems to be consistent with the expression pattern of the *aglB* gene, which is expressed on a wide range of carbon sources including monosaccharides, oligosaccharides, and polysaccharides, and the release of a small amount of galactose through the action of AglB is assumed to be the induction of other α-galactosidases [6].

This broad substrate selectivity could be attributed to the architecture of an active-site pocket. A three-dimensional structure of AglB has not been available, but it could be similar to that of *Trichoderma reesei* α-galactosidase (pdb identifiers, 1SZN and 1T0O). [12] *T. reesei* α-galactosidase belongs to the same cluster as AglB according to a phylogenetic analysis of GH27 enzymes by Fernández-Leiro *et al*. [13] The amino acid sequence of *T. reesei* α-galactosidase shares a 54% identity to that of AglB and

bears a discriminative long loop connecting β-strand 4 and α-helix 4. A protein fold recognition analysis by GenTHREADER (http://bioinf.cs.ucl.ac.uk/psipred/) indicated that AglB has a similar tertiary structure to that of *T. reesei* α-galactosidase. [14] *T. reesei* α-galactosidase has subsite −1 in a shallow active-site pocket. The α-galactoside is held there through numerous interactions including hydrogen bonds and van der Waals contacts. Meanwhile, subsite +1 is placed around the rim of the pocket and a few residues are relevant to the interaction. That is, *T. reesei* α-galactosidase seems to strictly recognize α-galactoside and loosely binds to the aglycone part. AglB can inherit this shallow active-site pocket and can recognize substrates similar to *T. reesei* α-galactosidase. In addition, a comparison of k_{cat}/K_m for the hydrolysis of natural substrates provides the substrate specificity of AglB, which prefers melibiose and galactomanno-oligosaccharides to raffinose and stachyose. The loose binding to the aglycone part may be an advantage when binding to branch substrates, but it will not be able to obtain the sufficient binding energy required for linear oligosaccharides, such as raffinose and stachyose.

Author contributions

Conceived and designed the experiments: M. Okuyama, H. Mori, S. Chiba, and A. Kimura. Performed the experiments: J. Liao, K. Ishihara, S. Iki, and Y. Yamori. Analyzed the data: M. Okuyama. Contributed reagents/materials/analysis tools: T. Tagami, Wrote the paper: M. Okuyama and A. Kimura.

Acknowledgements

We thank the staff of the Instrumental Analysis Division of the Creative Research Institution at Hokkaido University for the amino acid analysis. This work was

supported by JSPS KAKENHI Grant Number 26292049. The authors would like to thank Enago (www.enago.jp) for the English language review.

References

1. Dey PM. Biochemistry of plant galactomannans. Adv Carbohydr Chem Biochem. 1978;35:341–376.

2. Dea IA. Chemistry and interactions of seed galactomannans. Adv Carbohydr Chem Biochem. 1975;31:241–312.

3. de Vries RP, Visser J. Aspergillus enzymes involved in degradation of plant cell wall polysaccharides. Microbiol Mol Biol Rev. 2001;65:497–522.

4. Malgas S, van Dyk SJ, Pletschke BI. β-mannanase (Man26A) and α-galactosidase (Aga27A) synergism – a key factor for the hydrolysis of galactomannan substrates. Enzyme Microb Technol. 2015;70:1–8.

5. den Herder IF, Rosell AM, van Zuilen CM, et al. Cloning and expression of a member of the Aspergillus niger gene family encoding alpha-galactosidase. Mol Gen Genet. 1992;233:404–410.

6. de Vries RP, van den Broeck HC, Dekkers E, et al. Differential expression of three α-galactosidase genes and a single β-galactosidase gene from Aspergillus niger. Appl Environ Microbiol. 1999;65:2453–2460.

7. Ademark P, de Vries RP, Hagglund P, et al. Cloning and characterization of Aspergillus niger genes encoding an α-galactosidase and a β-mannosidase involved in galactomannan degradation. Eur J Biochem. 2001;268:2982–2990.

8. Kohrer K, Domdey H. Preparation of high–molecular weight RNA. Methods Enzymol. 1991;194:398–405.

9. Lin-Cereghino J, Wong WW, Xiong S, et al. Condensed protocol for competent cell

preparation and transformation of the methylotrophic yeast Pichia pastoris. Biotechniques. 2005;38:44.

10. Brumer H, Sims PF, Sinnott ML. Lignocellulose degradation by Phanerochaete chrysosporium: purification and characterization of the main α-galactosidase. Biochem J. 1999;339:43–53.

11. Feng S, Bagia, C, Mpourmpakis G. Determination of proton affinities and acidity contants of sugars. J Phys Chem A. 2013;117:5211–5219.

12. Golubev AM, Nagem RA, Brandao Neto JR, et al. Crystal structure of α-galactosidase from Trichoderma reesei and its complex with galactose: implications for catalytic mechanism. J Mol Biol. 2004;339:413–422.

13. Fernandez-Leiro R, Pereira-Rodriguez A, Cerdan ME, et al. Structural analysis of Saccharomyces cerevisiae α-galactosidase and its complexes with natural substrates reveals new insights into substrate specificity of GH27 glycosidases. J Biol Chem. 2010;285:28020–28033.

14. Lobley A, Sadowski MI, Jones DT. pGenTHREADER and pDomTHREADER: new methods for improved protein fold recognition and superfamily discrimination. Bioinformatics. 2009;25:1761–1767.

Figure Legends

Fig. 1. SDS-PAGE gel with Coomassie Brilliant Blue staining of the purified recombinant AglB.

Positions of Marker proteins (M) and molecular masses (kDa) are shown on the side. Lane 1, glycosylated protein as a broad band; lane 2, deglycosylated protein with endoglycosidase H. The band with a molecular mass of 29 kDa in lane 2 is endoglycosidase H.

Fig. 2. Enzyme-catalyzed hydrolysis of PNPG.

(A) pH dependence of the hydrolytic rate of 2 mM PNPG by rAglB. (B) Plots of reaction velocity ($v/[E]_0$) versus substrate concentration for hydrolysis of PNPG at pH 6.7 by rAglB. (C) pH dependence of k_{cat}/K_m for the hydrolysis of PNPG by rAglB.

Fig. 3. Kinetic scheme for substrate inhibition.

Scheme 1, Substrate inhibition caused by the formation of the dead-end ESS complex. Scheme 2, Substrate inhibition caused by the formation of the inert FS complex. ES, Michaelis complex; F, covalent intermediate; ESS, substrate-inhibited Michaelis complex; FS, substrate-inhibited covalent intermediate or transglycosylation complex;

P_1, *p*-nitrophenol; P_2, galactose; P_3, transglycosylation product.

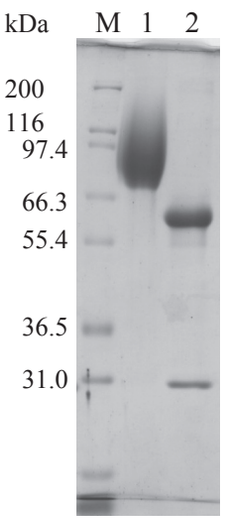

Fig. 1. Liao *et al*

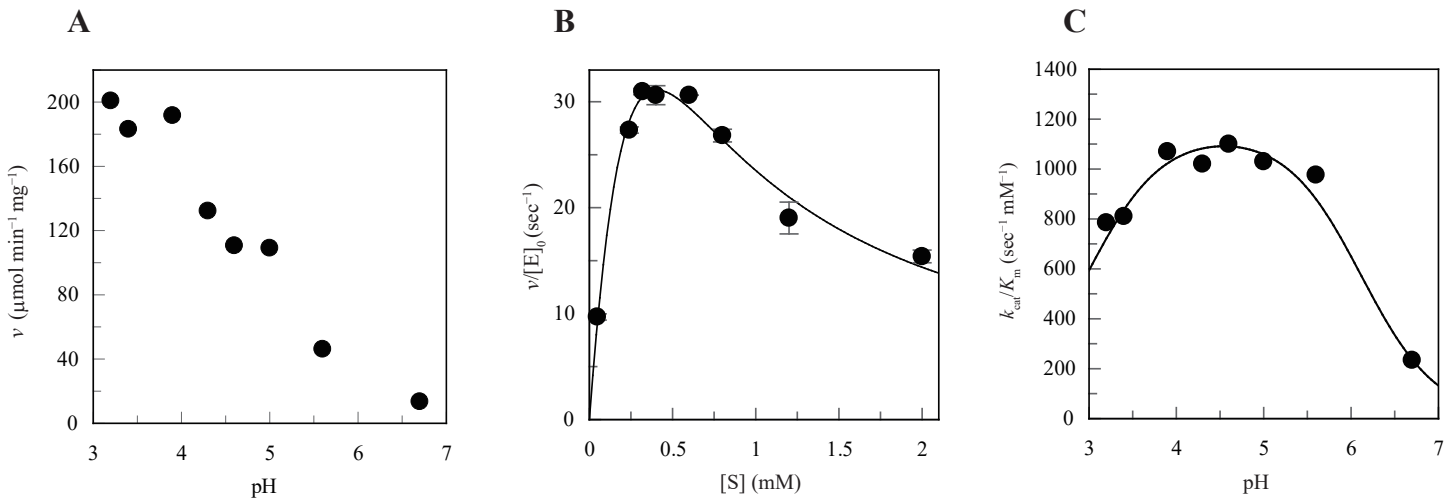

Fig. 2. Liao *et al*

Scheme 1

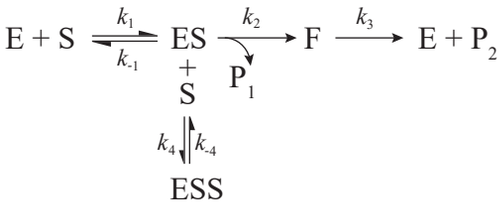

Scheme 2

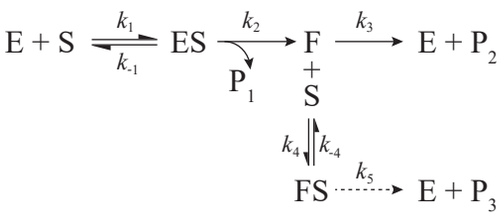

Fig. 3. Liao *et al*